Theoretical study of perpendicular giant magnetoresistance in multilayers

Julian Velev and Yia-Chung Chang

Department of Physics and Materials Research Laboratory, University of Illinois at Urbana-Champaign, Urbana, Illinois 61801
(Received 1 September 2000; revised manuscript received 31 October 2000; published 18 April 2001)

We investigate the conductance and giant magnetoresistance (GMR) in the current perpendicular-to-the-plane geometry in magnetic multilayers via a third-nearest-neighbor tight-binding model with s, p, and d orbitals. An iterative method is used to calculate the Green's function of the multilayer. The conductance, due to both minority and majority spin channels, is calculated in the ferromagnetic and antiferromagnetic configurations using the Landauer-Büttiker formula. Oscillations of GMR, both with spacer and magnetic layer thicknesses, are observed and the contributions to the conductance due to various extremal points on the Fermi surface are studied. Ballistic conductance and GMR are found to saturate very fast with the number of periods in the multilayer.

I. INTRODUCTION

The discovery of the giant magnetoresistance in Fe/Cr multilayers[1,2] has stimulated a great deal of research (for a review, see Refs. 3 and 4). The interest in the field has been fueled by the applications of giant magnetoresistance (GMR) for magnetic recording. A lot of work has been done both experimentally and theoretically. On the experimental side, GMR was first found in trilayers and multilayers with nearly perfect crystalline structure. Later, GMR was observed in sputtered samples and oscillations of GMR with changes in the thickness of the nonmagnetic layer were observed.[5] Most of the GMR measurements are done in the current-in-the-plane (CIP) geometry because the sample has macroscopic size and thus significant resistance. However, there are measurements of GMR in the current-perpendicular-to-the-plane (CPP) geometry,[6] and GMR observed in CPP geometry is often larger than GMR observed in CIP geometry. The temperature dependence of the CPP GMR in multilayers is also studied.[7,8]

The first theoretical works on GMR are based on the free-electron model and semi-classical treatment of transport.[9] This approach does not take into account the band structure of the materials and employs many phenomenological parameters. Spin-dependent scattering from the interfaces and the bulk is identified as the source of GMR. However, Schep, Kelly, and Bauer[10] showed that the observed values of GMR can be obtained from the band structure alone. They commented that although the transport in real samples is diffusive rather than ballistic, it is very improbable that the band-structure effects are completely subdued. This led to many calculations of GMR based on rigorous quantum theory of scattering. All methods utilize either the Kubo-Greenwood formula or the equivalent Landauer-Büttiker formula. The band structure is taken into account either *ab initio* or via tight-binding (TB) interpolation scheme. The *ab initio* method has been applied to pure multilayers,[10,11] multilayers with disorder[12] within the coherent potential approximation, and recently, spin-valve systems.[13] The main problem with this method is the computational overload that affects adversely the size of the systems that can be studied. The TB

method offers the convenience of taking the band structure as input and thus reducing the computational time. It is especially useful for multilayers because it discretizes the spatial continuum in a natural way. The method has been used by several groups so far. Tsymbal and Pettifor[14] used the full sp^3d^5 TB model to calculate GMR in infinite Co/Cu and Fe/Cr superlattices with fixed slab sizes. Mathon *et al.*[15] calculated GMR of a Co/Cu trilayer from the Kubo formula using full sp^3d^5 TB model. They studied the dependence of GMR from both magnetic and spacer layer thickness. In another paper Mathon[16] observed that ballistic conductance in multilayers saturates after a relatively small number of periods. Later, Sanvito *et al.*[17] studied GMR of finite Co/A and Ni/A (A=Cu, Ag, Pb, Au, and Pt) multilayers from the Landauer formula also using sp^3d^5 TB model. Another GMR calculation of Co/Cu trilayers was given by Zwierzycki and Krompiewski[18] using reduced sd^1 TB model and a simplifying assumption of a simple cubic lattice. Despite all the work done, little attention was paid to Fe/Cr multilayers where GMR was originally observed.[1] Furthermore, the experimental observation that GMR increases when one adds extra magnetic layers[2] and existing calculations,[16] point to the need for further study of the dependence of GMR on the number of periods in the multilayer.

The purpose of this work is to investigate the ballistic conductance and CPP GMR of finite Fe/Cr multilayers, and in particular, the dependence of GMR on the number of periods in the multilayer and layer thickness, taking into account the realistic band structures. The calculation is based on empirical third-nearest-neighbor tight-binding model with s,p,d orbitals, fitted to *ab initio* band structures of the constituent materials. Our main result is that the ballistic conductance and GMR saturate after a small number of periods (∼2–6) that agrees with the results of Ref. 16. However, our method differs in the calculation of the conductance and the Green's function (GF) that makes the agreement with Mathon even more significant. We calculate the conductance from the Landauer-Büttiker formula instead of the Kubo formula and we use an iterative method and self-energies to calculate the GF instead of a recursive method and the Dyson equation. We go a step further to show that the satu-

ration value of GMR is related to the strength of the inter-layer exchange coupling (IEC) because the same process prevents the conductance from saturating early.

This work is organized as follows. In Sec. II, we summarize the scattering formalism for the conductance. We, then, describe a method of calculating the GF of the multilayer by reconnecting the GF's of separate parts of the system. We state the expressions for the surface and slab GF's. In Sec. III, we present the results for the model system. In Sec. IV, we discuss possible implications of the results.

II. SCATTERING THEORY AND CONDUCTANCE

The calculation of the conductance is based on the Landauer formula, which was proposed by Landauer[19] for one-dimensional systems with a single channel, and later generalized for multiple dimensions and multiple channels.[20] For a multilayer sandwiched between two leads, the conductance is given by

$$\Gamma = \frac{e^2}{h} \int \bar{T}(E)\left(-\frac{\partial f_0}{\partial E}\right) dE, \qquad (2.1)$$

where f_0 is the equilibrium Fermi distribution function and $\bar{T}(E)$ is related to the Green's function of the system via[21]

$$\bar{T}(E) = \text{Tr}[\tilde{\Sigma}_L G^R(1,n)\tilde{\Sigma}_R G^A(1,n)], \qquad (2.2)$$

where $G^{R/A}(1,n)$ is the retarded/advanced GF matrix element between the first and the last principal layer of the sample and $\tilde{\Sigma} = i(\Sigma^R - \Sigma^A)$, where $\Sigma^R(\Sigma^A)$ is the retarded (advanced) self-energy operator that will be defined below [see Eq. (2.6)].

In the case of multilayers, the consecutive magnetic layers can be ferromagnetically or antiferromagnetically coupled. GMR is defined as the normalized difference between the conductance of ferromagnetic and antiferromagnetic configurations:

$$R_{\text{GMR}} = \frac{\Gamma_{\uparrow\uparrow} + \Gamma_{\downarrow\downarrow} - \Gamma_{\uparrow\downarrow} - \Gamma_{\downarrow\uparrow}}{\Gamma_{\uparrow\downarrow} + \Gamma_{\downarrow\uparrow}}. \qquad (2.3)$$

In the trilayer geometry, we have $\Gamma_{\downarrow\uparrow} = \Gamma_{\uparrow\downarrow}$ due to symmetry. This does not need to be true for a general multilayer system.

In the TB scheme the wave functions of the system are expressed in terms of orthogonal atomiclike orbitals. We choose the z axis to be perpendicular to the plane of the multilayer. Because the system has two-dimensional (2D) translational invariance in the plane, we can construct 2D Bloch sums out of our atomiclike orbitals, labeled by the in-plane wave vector $\mathbf{k}_\parallel$. For simplicity we introduce the *principal layer* (PL) in the usual way: each PL interacts only with itself and the adjacent PL's; and a PL is a unit cell for 1D translations normal to it. A PL can contain one or more atomic planes. A layer orbital associated with wave vector $\mathbf{k}_\parallel$ and the lth layer is defined as the following Bloch sum of the TB orbitals:

$$\langle \mathbf{r} | \mathbf{k}_\parallel ; \alpha, l \rangle = \sum_{\mathbf{R}_\parallel} e^{i\mathbf{k}_\parallel \cdot \mathbf{R}_\parallel} \phi_\alpha(\mathbf{r} - \mathbf{R}_\parallel - l R_z),$$

where $\mathbf{R}_\parallel$ is an in-plane lattice vector, R_z is distance between two consecutive layers, and $\phi_\alpha(\mathbf{r} - \mathbf{R})$ denotes a TB orbital within the unit cell. The index α is a composite label for both the orbital type of each atom and different atoms within the unit cell. The Hamiltonian matrix between the layer orbitals at mth and nth layer will be denoted as H_{mn} with the $\mathbf{k}_\parallel$ dependence left implicit. We use the standard two-center-integral approximation described by Slater and Koster.[22] The TB parameters are obtained by fitting the TB band structure to *ab initio* band structures.[23]

The system can be divided into three parts: the left lead, the multilayer slab, and the right lead. The corresponding GF's are denoted by G_L, G_S, and G_R, respectively. To connect the multilayer slab to the infinite leads, we have to define TB matrix elements in the interface region. As in typical empirical TB calculations, we take them to be the arithmetic average of the hopping integrals associated with the constituent materials on both sides of the interface. The matrix equation for the full GF of the system takes the form

$$\begin{vmatrix} G_L & G_{LS} & G_{LR} \\ G_{SL} & G_S & G_{SR} \\ G_{RL} & G_{RS} & G_R \end{vmatrix}$$

$$= \begin{vmatrix} (E1 - H_L) & H_{LS} & 0 \\ H_{SL} & (E1 - H_S) & H_{SR} \\ 0 & H_{RS} & (E1 - H_R) \end{vmatrix}^{-1}. \qquad (2.4)$$

If we do the inversion analytically, we can obtain the GF associated with the slab in terms of the self-energies that take into account the effects of coupling with the leads,
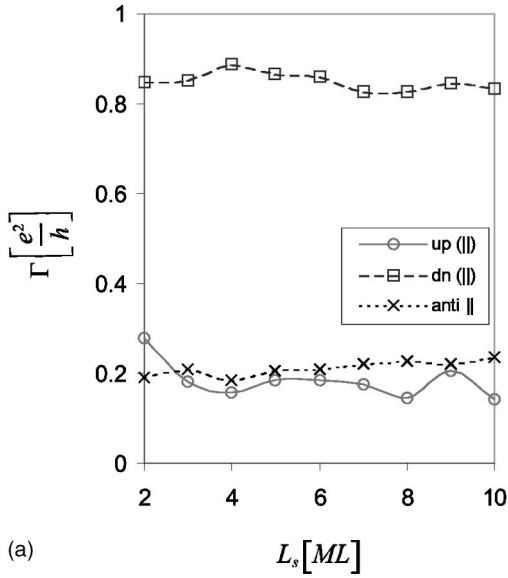
$$G_S = (E1 - H_S - \Sigma_L - \Sigma_R)^{-1}, \qquad (2.5)$$
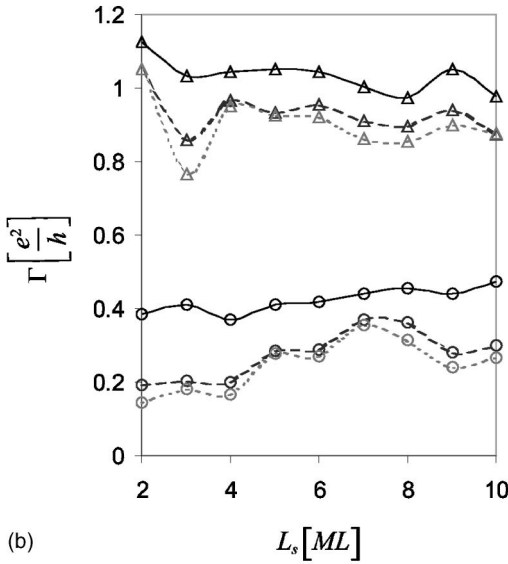
where the self-energies have the form

$$\Sigma_L = H_{SL} G_L H_{LS},$$

$$\Sigma_R = H_{SR} G_R H_{RS}. \qquad (2.6)$$

The Hamiltonian matrix for the multilayer slab has the form

$$H_S = \begin{vmatrix} H_0^{F1} & H_{-1}^{F1} & 0 & 0 & \cdots & 0 \\ H_1^{F1} & H_0^{F1} & H_{-1}^{F1-S1} & 0 & & 0 \\ 0 & H_1^{F1-S1} & H_0^{S1} & H_{-1}^{S1} & & 0 \\ 0 & 0 & H_1^{S1} & H_0^{S1} & & 0 \\ \vdots & & & & \ddots & \\ 0 & 0 & 0 & 0 & \cdots & H_0^{Fn} \end{vmatrix}, \qquad (2.7)$$
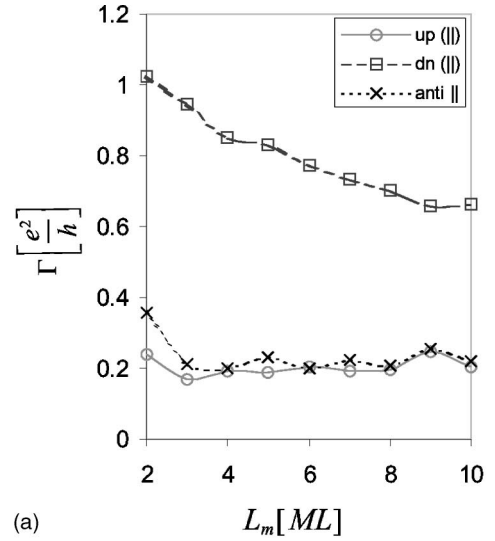
FIG. 1. Conductance (in units of e^2/h) vs spacer layer thickness in Fe/Cr(001) multilayers. The Fe layers are 4 ML thick (in this case 1 ML$=1.44$ Å). (a) Minority and majority spins in parallel configuration, either one in antiparallel configuration in a Fe/Cr(001) trilayer. (b) Parallel and antiparallel conductance in Fe/Cr(001) multilayers. The lines represent: solid, $N=2$; long dashes, $N=5$; dashes, $N=8$. Parallel conductance points are labeled by triangles, antiparallel by circles.

FIG. 2. Conductance (in units of e^2/h) vs magnetic layer thickness in Fe/Cr(001) multilayers. The Cr layer is 3 ML thick (in this case 1 ML$=1.44$ Å). (a) Minority and majority spins in parallel configuration, either one in antiparallel configuration in a Fe/Cr(001) trilayer. (b) Parallel and antiparallel conductance in Fe/Cr(001) multilayers. The lines represent: solid, $N=2$; long dashes, $N=5$; dashes, $N=8$. Parallel conductance points are labeled by triangles, antiparallel by circles.

where $F1$ is the first magnetic slab, $S1$ is the first nonmagnetic slab, etc.
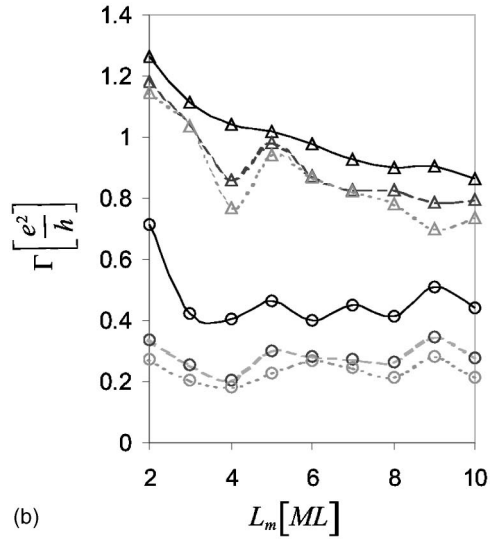
To treat the semi-infinite leads we need a more sophisticated technique. The starting point is the equation for the GF in TB representation

$$\bar{H}_{n,n+1}G_{n+1,n'}+\bar{H}_{n,n}G_{n,n'}+\bar{H}_{n,n-1}G_{n-1,n'}=-1,$$
(2.8)

where $\bar{H}=H-E1$ for brevity. We first calculate iteratively an object called *amplitude transfer matrix* (T), using the

method derived in Ref. 24. We then construct through it all GF matrix elements via the relations

$$G_{n+1,m}=TG_{n,m}(n>m),\quad G_{n-1,m}=\bar{T}G_{n,m}(n<m),$$

$$G_{n,m+1}=G_{n,m}S(n<m),\quad G_{n,m-1}=G_{n,m}\bar{S}(n>m),$$
(2.9)

where

$$S=\bar{H}_{-1}T(\bar{H}_1)^{-1},\quad \bar{S}=\bar{H}_1\bar{T}(\bar{H}_{-1})^{-1}.$$
(2.10)
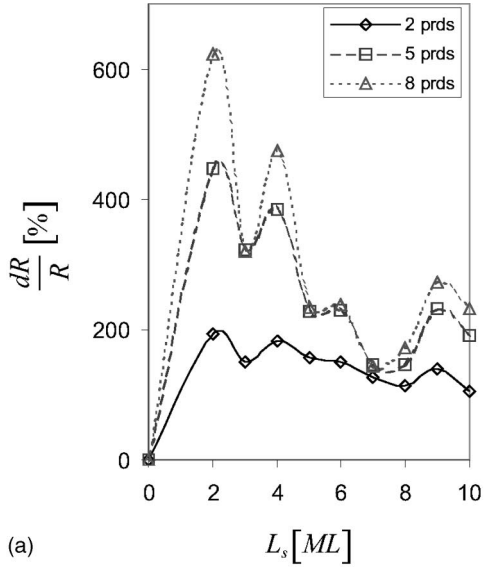
(a)
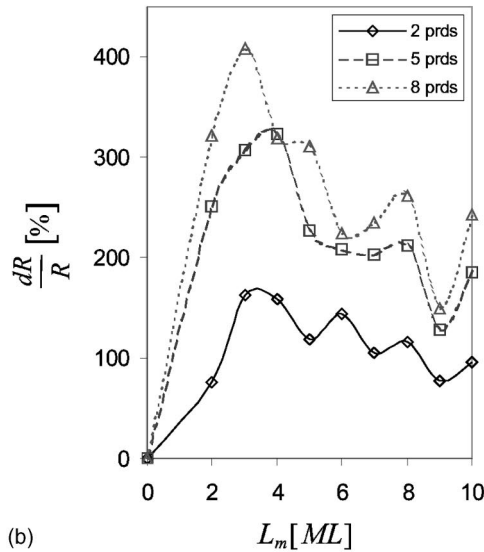
(b)

FIG. 3. (a) GMR vs spacer layer thickness in Fe/Cr(001) multilayers. The Fe layers are 4 ML thick (in this case 1 ML = 1.44 Å). (b) GMR vs magnetic layer thickness in Fe/Cr(001) multilayers. The Cr layers are 3 ML thick (in this case 1 ML = 1.44 Å).

Thus, the transfer matrices can be solved iteratively only with the knowledge of the Hamiltonian matrix elements.

Next, the GF's of the semi-infinite leads are obtained via

$$G_L = -(\bar{H}_0 + \bar{H}_{-1}T)^{-1}, \qquad (2.11)$$
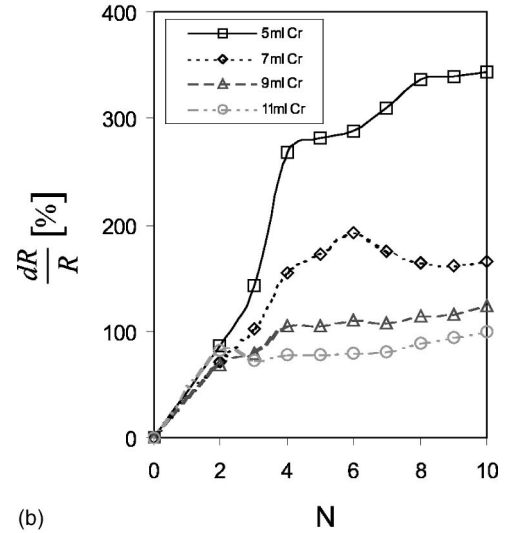
for the left surface, and

$$G_R = -(\bar{H}_0 + \bar{H}_1\bar{T})^{-1} \qquad (2.12)$$

for the right surface. We only need to evaluate the matrix elements of G_L and G_R in the interface principal layers.

Finally, the GF of the combined system (multilayer plus leads) is obtained via Eqs. (2.5) and (2.6). The most demanding operation in the whole calculation is the matrix inverse in
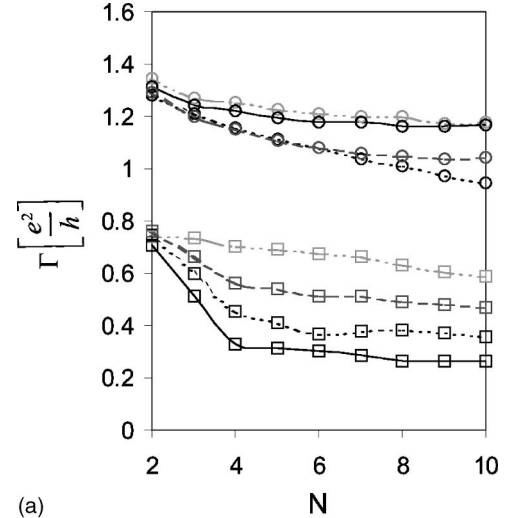
(a)

(b)

FIG. 4. (a) Parallel and antiparallel conductance vs number of periods in Fe/Cr(001) multilayers. (b) GMR vs number of periods in Fe/Cr(001) multilayers. Every period has 2 ML of Fe and N ML of Cr ($N = 5$, 7, 9, and 11).

Eq. (2.5), because the matrix tends to grow very large when one includes full set of orbitals, thick slabs, and many periods, as frequently needed in realistic calculations. To overcome this difficulty we use a modified Gauss elimination algorithm, utilizing the fact that the matrix is banded and we only need the matrix elements of G_S linking the two PL's at the left and right interface [see Eq. (2.2)].

III. DISCUSSION OF RESULTS

Using the results stated above we study the dependence of GMR on the number of periods in the multilayer as well as the individual layer thicknesses. We define the multilayer to be a sandwich of N magnetic layers of thickness L_m and $N - 1$ nonmagnetic (spacer) layers of thickness L_s in between. The whole stack is sandwiched between semi-infinite leads made of the nonmagnetic material. There are no impurities in the bulk and the interfaces are perfectly flat. First, we con-
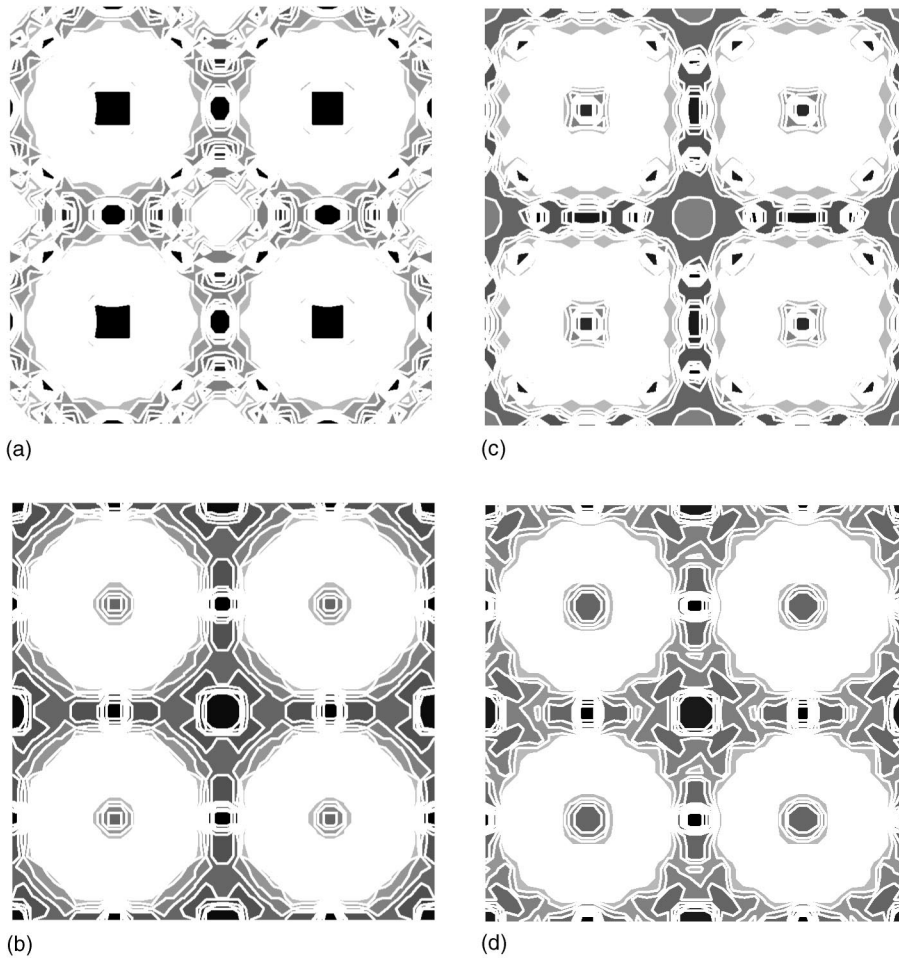
FIG. 5. Contributions to the conductance and GMR in a Fe/Cr(001) trilayer due to different $\mathbf{k}_{\parallel}$ in the surface Brillouin zone. The Fe is 4 ML and Cr is 3 ML thick. (a) Majority spin. (b) Minority spin. (c) Either spin in antiparallel configuration. (d) GMR. Darker areas indicate bigger contribution.

sidered the dependence of the conductance in Fe/Cr(001) multilayers on the Cr thickness (Fig. 1). The Fe layer thickness is fixed at 4 ML. Figure 1(a) shows the conductance in a trilayer ($N=2$) vs spacer layer thickness in ML. As expected, the conductance is dominated by the minority carriers that have transmission amplitude larger than the majority carriers due to their smaller density of states near the Fermi level. Figure 1(b) shows the overall conductance in parallel and anti-parallel configurations for several multilayers. With an increase of N two things happen: the conductance initially decreases and then saturates, and the quantum oscillations become more pronounced.

Second, we study the dependence of the conductance of the magnetic layer thickness (Fig. 2). The Cr layer thickness is fixed at 3 ML. Figure 2(a) shows the conductance in a trilayer as a function of the magnetic layer thickness. Figure 2(b) compares the overall conductance in several multilayers. Qualitatively, the behavior is very similar to Fig. 1. In ballistic regime the electrons propagate without scattering in the slabs so they see the difference between the magnetic and nonmagnetic material only at the interfaces. The oscillations in conductance are due to multiple scattering of the electrons in the multilayer. At certain thicknesses electrons form resonance states in the magnetic layer (as a result of quantum confinement) and thus do not contribute to the current appreciably.[25]

Third, we calculated GMR as a function of both the spacer and magnetic layer thicknesses (Fig. 3). Figure 3(a) shows GMR vs L_s for several multilayers, L_m is fixed to 4 ML. Figure 3(b) shows GMR vs L_m, L_s is fixed to 3 ML. We assume that consecutive magnetic layers are always antiferromagnetically aligned. However, in real systems this is only possible at certain spacer thicknesses. Methods for identifying when antiferromagnetic alignment naturally occurs have been well established.[26] In cases when antiferromagnetic alignment is not possible the antiferromagnetic conductance is not defined and GMR is by definition zero.

Next, we studied GMR as a function of the number of periods N in the multilayer with fixed thickness of each period (Fig. 4). Figure 4(a) shows the conductance vs N for several different L_s (L_m fixed at 2 ML). Figure 4(b) shows the correspondent GMR. We find that, initially, GMR increases very fast but approaches a constant value after a relatively small number of periods ($N \sim 2-6$). Also, the maximum value of GMR is inversely proportional to the Cr layer thickness and the saturation point is reached earlier for thicker Cr slabs. This is explained as follows: while the minority conductance is almost unaffected by the increased number of interfaces, the majority conductance (due to stronger scattering) dips sharply with the introduction of new interfaces, especially at small slab thicknesses. Knowing that the IEC strength decreases with the slab thickness,[26] we conclude that the same mechanism is responsible for both the

saturation value of GMR and the IEC strength.

We also investigated the contributions from various $\mathbf{k}_\parallel$ points in the surface Brillouin zone (SBZ) to the conductance and GMR. Because $\mathbf{k}_\parallel$ is a good quantum number, we can calculate conductance for different $\mathbf{k}_\parallel$ and then sum them up to get the total conductance. The results we obtained for an Fe/Cr/Fe(001) trilayer (with $L_s = 3$, $L_m = 4$ ML) are shown in Fig. 5. One can easily see the similarities with the Fermi surface of Cr in (001) orientation. Figure 5(a) and 5(b) show the majority and minority conductance in SBZ, respectively. We find that for the majority-spin channel the dominant contributions are from electrons with $\mathbf{k}_\parallel$ near the extremal vectors $\bar{N}_2$ with coordinates $(\pm 0.5, \pm 0.5)2\pi/a$ and $\bar{N}_1$ with coordinates $(0, \pm 0.5)2\pi/a$ and $(\pm 0.5,0)2\pi/a$, while for the minority channel, electrons with $\mathbf{k}_\parallel$ near the zone center contribute the most. Figure 5(c) shows the contributions to the antiparallel conductance due to different $\mathbf{k}_\parallel$ in SBZ. In this case many extremal vectors including $\bar{N}_1$, $\bar{N}_2$, and $\bar{L}$ [with coordinates $(0, \pm 0.29)2\pi/a$ and $(\pm 0.29,0)2\pi/a$] all contribute evenly to the conductance because what are minority electrons in the one ferromagnetic layer become majority electrons in the other. Figure 5(d) shows the contributions to GMR due to different $\mathbf{k}_\parallel$ in SBZ. We find that the most dominant contributions are from electrons with $\mathbf{k}_\parallel$ near the zone center, while secondary contributions are from the $\bar{N}_1$ extremal points.

Finally, there has been considerable interest in the temperature dependence of GMR. Our calculation, using the finite-temperature Landauer formula, predicts a weak temperature dependence of GMR, while the experimental observation indicates a strong decay of GMR signal as temperature increases.[7] This behavior is analyzed extensively in the literature[27,28,8] and it is attributed primarily to thermal excitation of magnons.

IV. CONCLUSION

We presented a theoretical study of GMR of Fe/Cr(001) multilayers. We examined the dependence of GMR on the number of periods and the thicknesses of magnetic and spacer layers. Oscillatory behaviors in the thickness dependence of GMR due to quantum interference are found, which are consistent with previous studies. We find that the oscillatory behavior in GMR as a function of the slab thicknesses is related to the similar oscillatory behavior in IEC. The MR effect calculated with s or sp orbitals only is found to be very small. This leads to the conclusion that GMR is mainly due to the sp-d hybridization. Thus, calculations based on free electron model or TB model with s and p orbitals only cannot adequately describe this effect. We also calculated the contribution to the conductance from various points in the SBZ, for both minority and majority electrons. The extremal points in the BZ are found to play a more important role in producing GMR than other points. GMR of multilayers increases with the multilayer size but saturates at a relatively small size. The saturation value of GMR is found to be proportional to the IEC strength. The model does not adequately describe the observed temperature dependence of GMR. This is expected because the mechanisms of electron-magnon and electron-phonon scattering are not included. However, our calculations show that the observed magnitudes of GMR can be adequately described from the band structure of the constituent materials. For full understanding of the observed GMR and conductance one has to consider scattering from impurities and interface roughness. For adequate description of the finite temperature behavior, electron-lattice and electron-electron interactions must also be included.

[1] M. N. Baibich, J. M. Broto, A. Fert, F. Nguyen Van Dau, F. Petroff, P. Etienne, G. Creuzet, A. Friederich, and J. Chazelas, Phys. Rev. Lett. **61**, 2472 (1988).

[2] G. Binasch, P. Grunberg, F. Saurenbach, and W. Zinn, Phys. Rev. B **39**, 4828 (1989).

[3] P. M. Levy, Solid State Phys. **47**, 367 (1994).

[4] M. Gijs and G. Bauer, Adv. Phys. **46**, 285 (1997).

[5] S. S. P. Parkin, N. Moore, and K. P. Roche, Phys. Rev. Lett. **64**, 2304 (1990).

[6] W. P. Pratt, S.-F. Lee, J. M. Slaughter, R. Loloee, P. A. Schroeder, and J. Bass, Phys. Rev. Lett. **66**, 3060 (1991).

[7] M. A. M. Gijs, S. K. J. Lenczowski, and J. B. Giesbergs, Phys. Rev. Lett. **70**, 3343 (1993).

[8] M. A. M. Gijs, S. K. J. Lenczowski, R. J. M. van de Veerdonk, J. B. Giesbers, M. T. Johnson, and J. B. F. van de Stegge, Phys. Rev. B **50**, 16 733 (1994).

[9] T. Valet and A. Fert, Phys. Rev. B **48**, 7099 (1993).

[10] K. Schep, P. Kelly, and G. Bauer, Phys. Rev. Lett. **74**, 586 (1995); Phys. Rev. B **57**, 8907 (1998).

[11] W. H. Butler, X.-G. Zhang, D. M. C. Nicholson, and J. M. MacLaren, Phys. Rev. B **52**, 13 399 (1995).

[12] C. Blaas, P. Weinberger, L. Szunyogh, P. M. Levy, and C. B. Sommers, Phys. Rev. B **60**, 492 (1999).

[13] R. H. Brown, D. M. C. Nicholson, W. H. Butler, X.-G. Zhang, W. A. Shelton, T. C. Schulthess, and J. M. MacLaren, Phys. Rev. B **58**, 11 146 (1998).

[14] E. Yu. Tsymbal and D. G. Pettifor, Phys. Rev. B **54**, 15 314 (1996).

[15] J. Mathon, A. Umerski, and M. Villeret, Phys. Rev. B **55**, 14 378 (1997).

[16] J. Mathon, Phys. Rev. B **55**, 960 (1997).

[17] S. Sanvito, C. J. Lambert, J. H. Jefferson, and A. M. Bratkovsky, Phys. Rev. B **59**, 11 936 (1999).

[18] M. Zwierzycki and S. Krompiewski, J. Magn. Magn. Mater. **202**, 150 (1999).

[19] R. Landauer, IBM J. Res. Dev. **1**, 233 (1957).

[20] E. N. Economou and C. M. Soukoulis, Phys. Rev. Lett. **46**, 618 (1981); D. S. Fisher and P. A. Lee, Phys. Rev. B **23**, 6851 (1981); also a good review A. D. Stone and A. Szafer, IBM J. Res. Dev. **32**, 384 (1988).

[21] S. Datta, *Electronic Transport in Mesoscopic Systems* (Cambridge University Press, Cambridge, England, 1997).

[22] J. Slater and G. Koster, Phys. Rev. **94**, 1498 (1954).

[23] D. Papaconstantopoulos, *Handbook of the Band Structure of Elemental Solids* (Plenum, New York, 1986).

[24] M. P. Lopez-Sancho, J. M. Lopez-Sancho, and J. Rubio, J. Phys. F: Met. Phys. **14**, 1205 (1984); **15**, 851 (1985).

[25] B. Lee and Y. C. Chang, Phys. Rev. B **54**, 13 034 (1996).

[26] L. Tsetseris, B. C. Lee, and Y. C. Chang, Phys. Rev. B **55**, 11 586 (1997); Phys. Rev. B **56**, R11 392 (1997), and references therein.

[27] D. L. Mills, A. Fert, and I. A. Campbell, Phys. Rev. B **4**, 196 (1971).

[28] J. E. Mattson, M. E. Brubaker, C. H. Sowers, M. Conover, Z. Qiu, and S. D. Bader, Phys. Rev. B **44**, 9378 (1991).